Catalysis Letters
https://doi.org/10.1007/s10562-018-2354-z

Nanohybrid Complexes with Molybdenyl Acetylacetonate, Schiff Base and Lacunary Keggin-Type Polyoxometalates: Synthesis and Catalytic Epoxidation of Olefins in the Presence of tert-Butyl Hydroperoxide

Samira S. Hosseinyzade[1] · **Farrokhzad M. Zonoz**[1] · **Bahram Bahramian**[2]

Received: 27 December 2017 / Accepted: 10 March 2018

Abstract

Two new nanohybrid compounds as heterogenous catalyst were prepared by reaction of Lacunary Keggin-type polyoxometalate compounds ($[SiW_{11}O_{39}]^{8-}$ and $[PW_{11}O_{39}]^{7-}$), molybdenyl acetylacetonate $[MoO_2(acac)_2]$ and ethylenediamine (en), (**1** and **2** respectively) species and characterized by elemental analysis and various routine techniques. The catalytic activities of these nanocatalysts examined for the epoxidation of linear, cyclic and phenyl-substituted olefins using tert-Butyl hydroperoxide (tert-BuOOH) as oxidants. The synergistic effect between molybdenyl acetylacetonate complex and lacunary Keggin-type polyoxometalate plays an important role in the promotion of catalytic activity. The catalysts were recovered and reused at least six times without obvious losing of activity and the yields for catalyst recovery are all above 91%.

Graphical Abstract

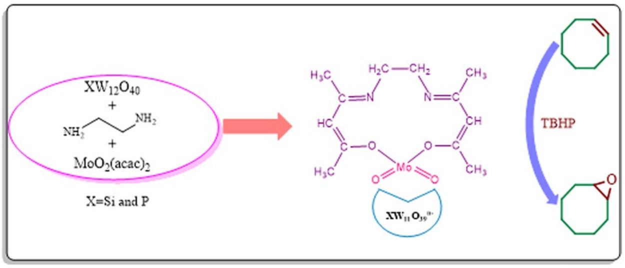

Keywords Keggin-type polyoxometalates · Molybdenyl acetylacetonate · Schiff base · Olefin · Epoxidation · Nanohybrid

1 Introduction

The preparations of new heterogeneous catalysts for selective oxidation of organic compounds are currently a notable assay purpose [1–5]. Heterogeneous catalysts have significant advantages over homogeneous catalysts such as stability, facility of separation, and reusability [6]. The oxidation of alkenes is a considerable process in the chemical and petrochemical industries [7, 8], because these compounds are greatly used for the synthesis of a variety of organic compounds like resins, surfactants, paints and are intermediates in pharmaceutical synthesis [9].

Polyoxometalates (POMs) are soluble anionic metal-oxide clusters with oxygen-rich surface, the intense tendency for coordination and potential applications in many fields such as catalysis, ion exchange, magnetism, photochemistry and material science [10–20]. Using POMs as acid and oxidation catalysts is one of the important applications of these compounds [21, 22]. Silicotungstic acid ($H_4SiW_{12}O_{40}$), phosphotungstic acid ($H_3PW_{12}O_{40}$) and their transition metal substituted of mono-defect fragments with Keggin structure

---

✉ Farrokhzad M. Zonoz
f.zonoz@hsu.ac.ir

[1] Department of Chemistry, Hakim Sabzevari University, Sabzevar 96179-76487, Iran

[2] College of Chemistry, Shahrood University of Technology, Shahrood 36155-316, Iran

have attracted much attention as oxidation catalysts due to the redox and acid feature and structural characteristics [23–29]. However, these compounds are soluble in polar solvents and therefore, using these compounds as a catalyst is associated with some restrictions [30, 31].

Nowadays, POMs attract much attention as building blocks for reaction with organic ligands due to their interesting structures [32–34]. They are great models for making hybrid compounds, which in recent years the notable attempt has been assigned to the design of nanostructured hybrid POMs [35–37]. Preparation of nanosized hybrid polyoxometalates increases the porosity of the structure and surface area. Moreover, solubility in polar solvent of these compounds also disappears due to incorporation of organic ligands as hydrophobic groups [38]. These compounds are new types of POM-based catalysts having great potential in heterogeneous catalysis in contrast to supported heterogeneous catalysts. The significant problem in supported catalysts is created by a poor connection between the polyoxometalates and the supports that causes loading these compounds by the solvent [39–41].

In this paper, we have successfully synthesized two new nanostructure organic–inorganic hybrid compounds with the sol–gel method, which characterized by instrumentals techniques. Then, we have used this nanohybrid polyoxometalates as heterogeneous catalyst for epoxidation of olefins using tert-Butyl hydroperoxide as oxidants. Furthermore the effects of different solvents, temperatures, content of oxidant and catalyst, and time on the activity of the catalysts on cis-cyclooctene as model reaction were investigated. And finally epoxidation of several olefins including linear, cyclic and phenyl-substituted olefins with tert-Butyl hydroperoxide as oxidant were investigated.

2 Experimental

2.1 General

All reagents were commercially obtained and used without any further purification. [$MoO_2(acac)_2$] was prepared by the literature methods and identified by Fourier transform infrared (FT-IR) spectroscopy [42]. FT-IR spectra were obtained using KBr pellets on a Shimadzu 8400S FT-IR spectrometer in the range of 4000–400 cm^{-1}. The elemental analyses of carbon, hydrogen, and nitrogen were determined by a Perkin-Elmer CHN analyzer. The ICP analyses were performed by an ICP-Spectrociros CCD instrument. Gas chromatography (GC) was accomplished by a Shimadzu GC-16A instrument using a 2 m column, packed with silicon DC-200. X-ray powder diffraction (XRD) patterns were obtained by using Phillips PW-1800 or STOE diffractometer with Cu Kα radiation. UV–Vis spectra were recorded on a Perkin-Elmer Lambda 25 spectrophotometer. Thermogravimetric analysis (TGA) analyses were carried out on Netzsch—TGA 209 F1 instrument under nitrogen atmosphere with 30 mL min^{-1} flow rate. The temperature range was 20–700 °C with the heating rate of 10 °C min^{-1}. Field emission scanning electron microscopy (FESEM) equipped by EDS microanalysis was done with MIRA3TESCAN-XMU instrument.

2.2 Methods

2.2.1 Preparation of Mono-lacunary Silicotungstate Molybdenyl Acetylacetonato Schiff Base (1)

A 0.719 g of $H_4SiW_{12}O_{40}$ (0.25 mmol) was dissolved in minimum of distilled water, and during stirring a 0.066 mL of ethylenediamine (1 mol) was added with vigorous stirring. After 30 min the methanol solution of 0.33 g [$MoO_2(acac)_2$] (1 mmol) was added and the mixture was refluxed for 5 h at 80 °C. The light green color precipitate was filtered, washed with methanol, and dried at 80 °C. IR (KBr disk): 3330, 3263, 3188, 3103, 2926, 1604, 1533, 1442, 1323, 914, and 788 cm^{-1}. Elemental analysis results showed: C, 5.85; H, 1.03; Mo, 3.10; N, 2.75; Si, 0.91; W, 64.37%. Calculations for $C_{15}H_{34}MoN_6O_{43}SiW_{11}$ (3132.51): C, 5.75; H, 1.08; Mo, 3.06; N, 2.68; Si, 0.90; W, 64.56%.

2.2.2 Preparation of Mono-lacunary Phosphotungstate Molybdenyl Acetylacetonato Schiff Base (2)

According to the above method the compound of **2** can be synthesized as similar method in which the $H_3PW_{12}O_{40}$ was used instead of $H_4SiW_{12}O_{40}$. IR (KBr disk): 3350, 3270, 3193, 3105, 2933, 1620, 1592, 1533, 1436, 1317, 1080, 973, 885, and 796 cm^{-1}. Elemental analysis results showed: C, 6.16; H, 1.25; Mo, 3.08; N, 2.87; P, 0.90; W, 63.88%. Calculations for $C_{15}H_{34}MoN_6O_{43}PW_{11}$ (3135.51): C, 5.74; H, 1.08; N, 2.68; W, 64.50; Mo, 3.06; P, 1.00%.

2.2.3 General Procedure for the Epoxidation of Alkenes

All reaction performed in 10 mL round bottom flask equipped with a magnetic stirrer bar and a condenser under similar refluxed conditions. The mixture of alkene (0.5 mmol), catalyst **1** (10 mg, 3 mmol) and for catalyst **2** (20 mg, 6 mmol), and tert-BuOOH (0.4 mL) were refluxed in 1,2-dichloroethane as solvent. The progress of reaction was monitored by gas chromatography analysis. Blank experiments were also performed in the absence of catalyst under the same experimental conditions. Since different alkenes have various reactivity toward oxidation the reactions were continued until no further progress was observed.

3 Results and Discussion

3.1 Synthesis Compounds of 1, and 2

Compounds **1** and **2** were synthesized from the reaction between Keggin-type POMs, ethylene diamine and molybdenyl acetylacetonate. By addition ethylenediamine to POMs solution, the pH of media increases and then Keggin-type POMs changing to mono-lacunary species. In 2014, Memon et al. was reported preparation of a Schiff's base in the reaction of acetyl acetone and ethylene diamine [43]. Therefore a combination of molybdenyl acetylacetonate Schiff base complex and mono-lacunary POMs can be considered in formation of **1** and **2** nanocatalysts (Scheme 1).

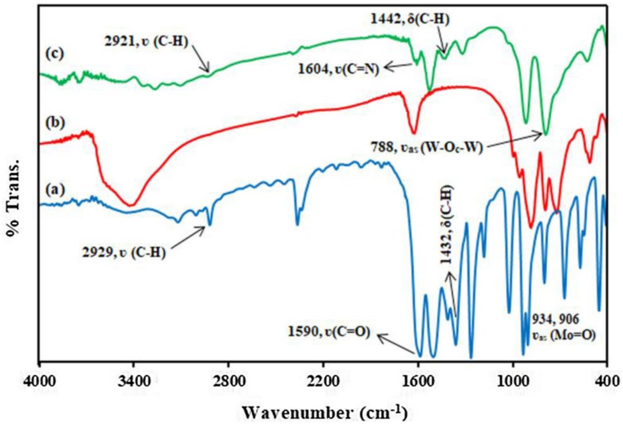

Fig. 1 The FT-IR spectra of *a* $[MoO_2(acac)_2]$, *b* $[SiW_{11}O_{39}]^{8-}$ and *c* compound **1**

3.2 Characterization of Mono-lacunary Polyoxometalate Molybdenyl Acetylacetonato Schiff Base Nanocatalysts (1, and 2)

3.2.1 FT-IR Analysis

The FT-IR spectrum of $[MoO_2(acac)_2]$, $[SiW_{11}O_{39}]^{8-}$, and **1** are shown in Fig. 1. The characteristic peaks at 2929, 1590, 1363, 934, and 906 cm^{-1} in $[MoO_2(acac)_2]$ spectrum (Fig. 1a) are attributed to υ (C–H), υ (C=O), δ (C–H), and υ_{as} (Mo=O) respectively [44]. The $[SiW_{11}O_{39}]^{8-}$ POM spectrum (Fig. 1b) shows five characteristic peaks at 995 [υ_{as} (Si–O)], 956 [υ_{as} (W–O$_t$)], 887 [υ_{as} (W–O$_b$–W)], 792 and 721 [υ_{as} (W–O$_c$–W)] cm^{-1} [45]. In the FT-IR spectrum of **1** (Fig. 1c), the characteristic peaks of $[MoO_2(acac)_2]$, $[SiW_{11}O_{39}]^{8-}$ and Schiff base can be seen. A very interesting point in this spectrum is related to a new peak at 1604 cm^{-1}, [υ (C=N)], which represents the formation of the bond between carbon and nitrogen atoms. This band may be attributed to the existence of imine group (Schiff base) in **1** which more specific in compound **2** [46]. In comparison of free $[MoO_2(acac)_2]$, the υ (C=O) peak of **1** overlap with ν (C=N) band and cannot be seen. In the range of 960–700 cm^{-1}, the peaks of $[MoO_2(acac)_2]$ and $[SiW_{11}O_{39}]^{8-}$ were overlap and υ_{as} (W–O$_c$–W) peaks is well seen.

The FT-IR spectrum of **2** (Fig. 2) is similar to compound **1**. The characteristic peaks of $[MoO_2(acac)_2]$,$[PW_{11}O_{39}]^{7-}$ anions and imine group can be seen in this spectrum. With increasing symmetry of $[PW_{11}O_{39}]^{7-}$ by filling the cavity with Schiff base ligand, the υ_{as} (P–O) of **2** shows one peak at 1080 cm^{-1} [45].

3.2.2 XRD Analysis

Figure 3 shows the XRD patterns of $[SiW_{11}O_{39}]^{8-}$, $[MoO_2(acac)_2]$, and **1**. The hybrid material reveals different structure compared to pure POM and $[MoO_2(acac)_2]$ compounds. The Keggin structure shows two typical reflexing area in XRD patterns ($2\theta = 2°–10°$ and $25°–35°$) [24]. According to the XRD pattern, **1** has a crystal structure after metal loading. A comparison of XRD patterns of

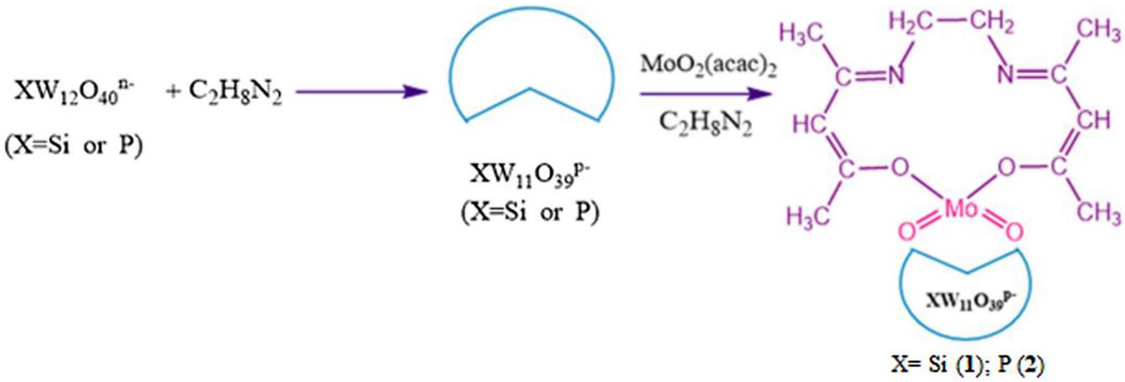

Scheme 1 Reaction scheme for the synthesis of **1** and **2** nanocatalysts

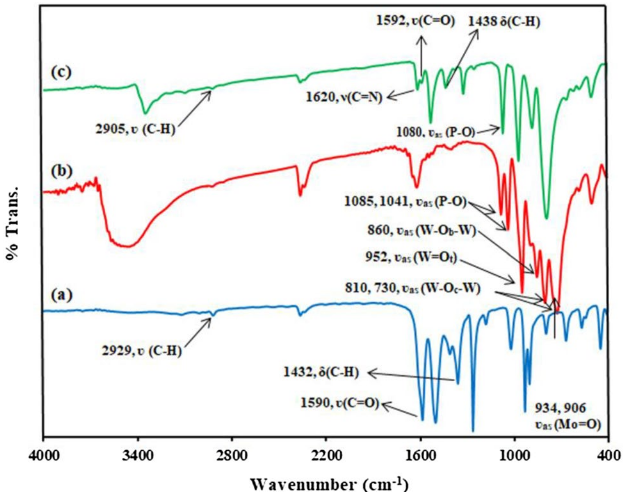

Fig. 2 The FT-IR spectra of *a* $[MoO_2(acac)_2]$, *b* $[PW_{11}O_{39}]^{7-}$ and *c* compound **2**

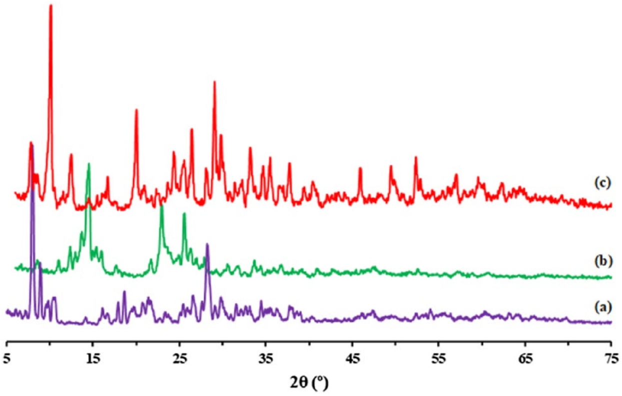

Fig. 3 XRD pattern of *a* $[SiW_{11}O_{39}]^{8-}$, *b* $[MoO_2(acac)_2]$ and *c* compound **1**

$[SiW_{11}O_{39}]^{8-}$, $[MoO_2(acac)_2]$, and catalyst **1** shows that the structure of primary polyoxometalate has been maintained during reaction. The structure of $[MoO_2(acac)_2]$ is largely altered and the intensity of its characteristic diffractions ($2\theta = 10°–20°$) decreases, which indicates the conversion of its structure and creation of a new composition like Schiff base complex in **1**. By using Williamson–Hall equation, the average particle size of the particles is of one has been estimated about 38 nm [47].

The XRD patterns of $[PW_{11}O_{39}]^{7-}$, $[MoO_2(acac)_2]$ and **2** are shown in Fig. 4. This XRD pattern shows similar results in the case of crystal structure and existence of polyoxometalate in compound **2**. By using similar calculations, the average size of the particles is estimated about 50 nm [47].

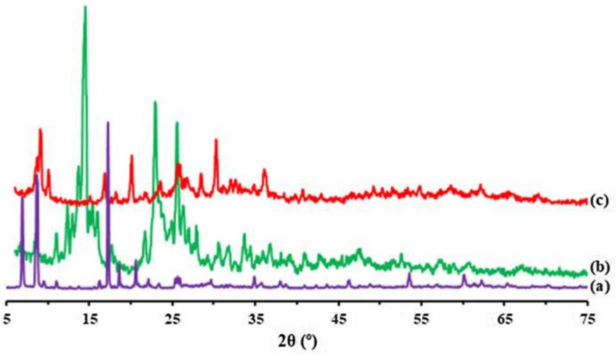

Fig. 4 XRD pattern of *a* $[PW_{11}O_{39}]^{7-}$, *b* $[MoO_2(acac)_2]$ and *c* compound **2**

3.2.3 FESEM Images

The FESEM images of compound **1** and **2** are shown in Fig. 5. These two compounds have a regular structure. This images confirmed that $[MoO_2\ (acac)_2]$ has been successfully supported on POMs. The results show that **1** possesses rod-like (particle size in the range of 84–108 nm) and spherical shape (particle size in the range of 36–40 nm) particles (Fig. 5b). According to this figure, the morphology of **1** can be considered as corn-like. This result is consistent with XRD data. The size of particles is estimated to be 30–60 nm for compound **1**, and 50–70 nm for compound **2**. The results of FESEM and XRD techniques are in good agreement with each other.

3.2.4 EDX Spectra

Energy dispersive X-ray analysis (EDX) is a very good technique for achieving data about the elemental composition of compounds. EDX analysis of **1** and **2** indicates the presence of C, N, O, Si, P, Mo, and W elements (Fig. 6). Based on these results, it is demonstrated the proposed structure of **1** and **2** nanocatalysts (Scheme 1).

3.2.5 UV Analysis

The UV–Vis spectra of $[MoO_2(acac)_2]$, $H_4SiW_{12}O_{40,}$ **1**, $H_3PW_{12}O_{40}$, and **2** are shown in Fig. 7. As shown in Fig. 7A a, B a, the characteristic absorption peaks at 263 and 256 nm for $H_4SiW_{12}O_{40}$ and $H_3PW_{12}O_{40}$ respectively, are attributed to the oxygen-to-metal (O → W) charge-transfer bands of Keggin anions [48]. As can be seen in this figure $[MoO_2(acac)_2]$ has a peak at 271 nm (Fig. 7A b, B b), which is attributed to the O (pπ) → Mo (dπ) charge transfer transition [49]. This peak is shifted to 321 and 315 nm in the **1** and **2** compounds (Fig. 7A c, B c). This

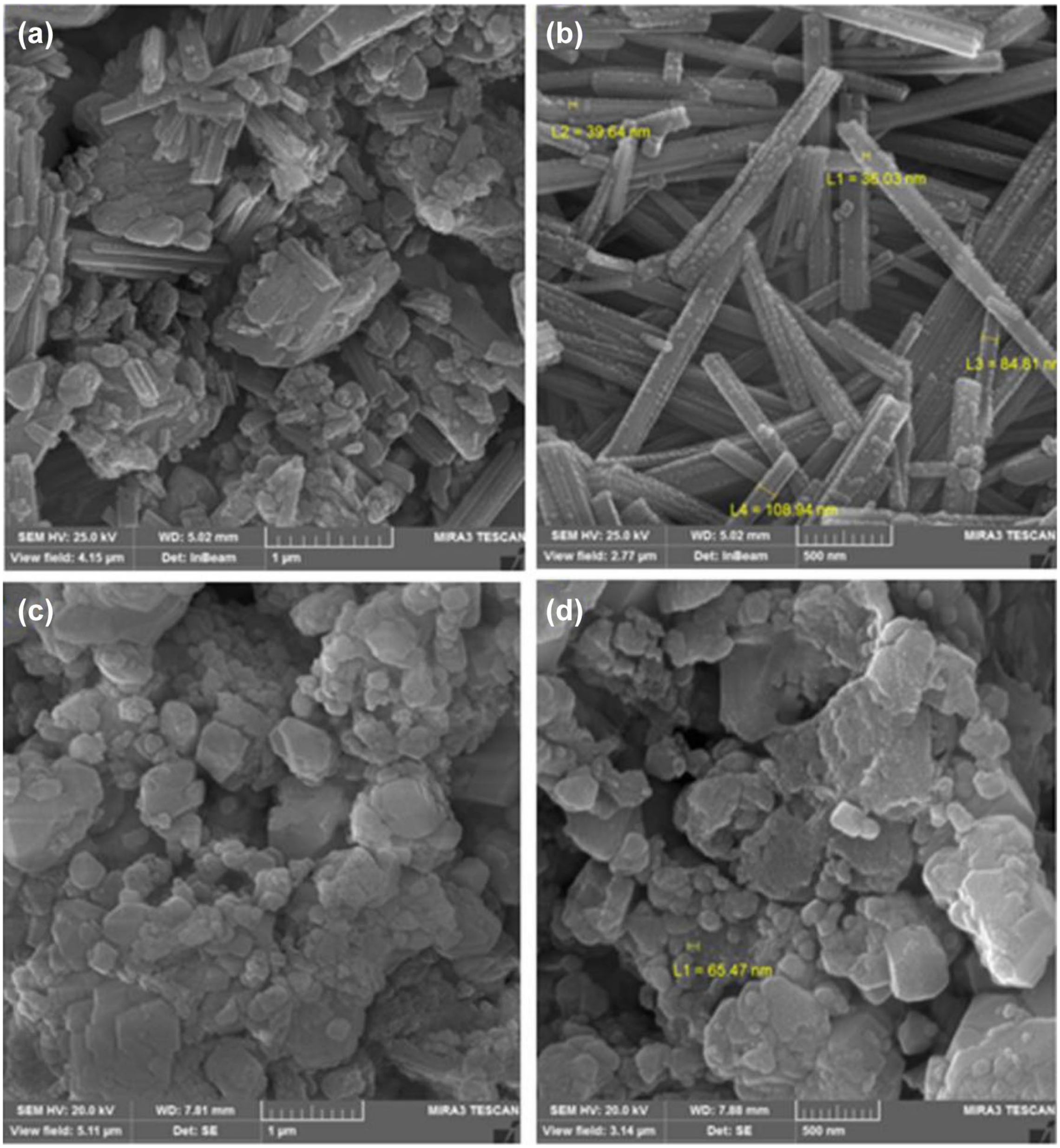

Fig. 5 FESEM images of **a, b 1** and **c, d 2** nanocatalysts

suggests an intramolecular interactions between POMs and [$MoO_2(acac)_2$].

3.2.6 DSC-TGA Analysis

The DSC-TGA curve of **1** (Fig. 8) was shown five step weight loss in the temperature range of 20–1000 °C. The first and second weight losses (4.61%) between 100 and 300 °C correspond to the removal of imine groups in Schiff base in two steps (Calc. 5.36%). The third and fourth weight losses (14.1%) exhibits in the temperature range of 320–550 °C is attributed to decomposition of molybdenyl acetylacetonate in **1** (Calc. 15.7%). The final weight loss step (14.8%) is attributed to decomposition of silicotungstate that occurs above 550 °C (Calc. 12.4%).

The DSC-TGA curve of **2** was shown in Fig. 9. This curve shows three remarkable steps in 20–1000 °C. The weight loss between 100 and 400 °C (6.1%) cab be attributed to the removal of imine groups (Calc. 5.36%). The removal of molybdenyl acetylacetonate and oxides of tungsten, phosphorus, and molybdenum oxides occurs between 400 and 1000 °C (24.2%) which nearly in accordance with the calculated values (27.9%).

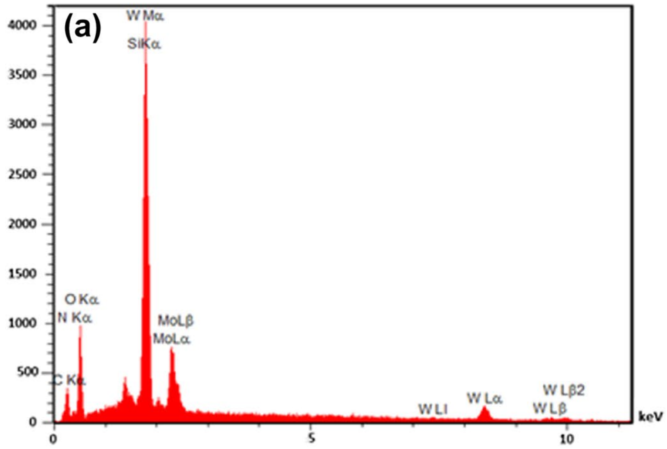

Fig. 6 The EDX spectra of **a** compound **1** and **b** compound **2**

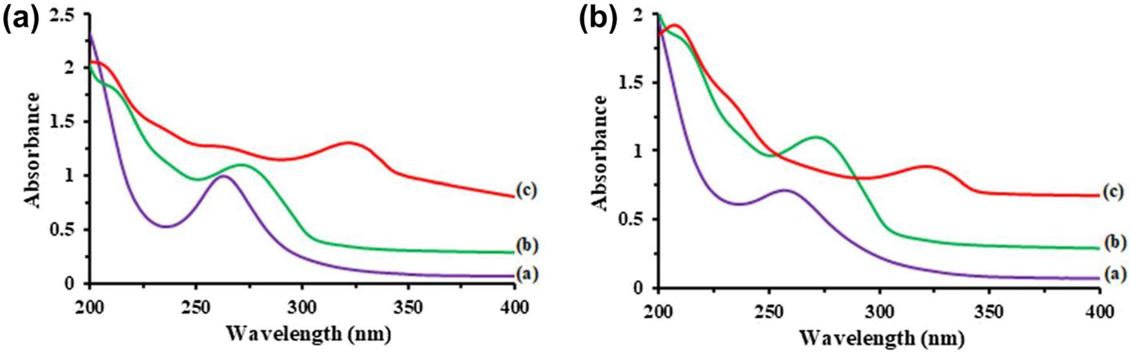

Fig. 7 UV–Vis spectra of **A** *a* $H_4SiW_{12}O_{40}$, *b* $[MoO_2(acac)_2]$ and *c* **1**. **B** *a* $H_4PW_{12}O_{40}$, *b* $[MoO_2(acac)_2]$ and *c* **2**

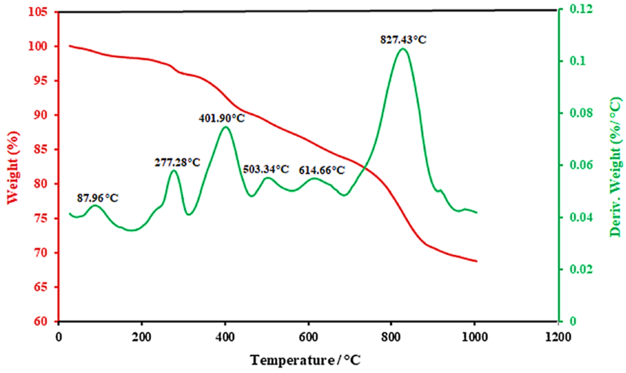

Fig. 8 DSC-TGA analysis of **1**

The results of FT-IR spectra, XRD patterns and DSC-TGA analysis can be confirm the proposed structure (Scheme 1).

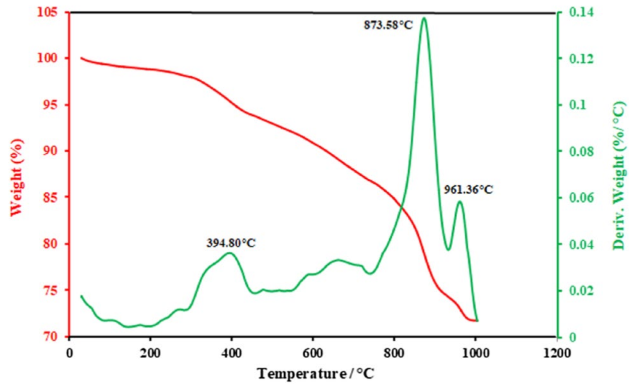

Fig. 9 DSC-TGA analysis of **2**

3.3 Catalytic Applications of 1 and 2 in the Epoxidation of Alkenes

The catalytic application of **1** and **2** nanoparticles in the epoxidation of alkenes using of tert-BuOOH as oxidant was investigated. Initially, in order to investigation of catalyst effect, the oxidation of cis-cyclooctene (as model reaction)

Table 1 Epoxidation of cis-cyclooctene at refluxed conditions

Entry	Catalyst (mg)	Solvent[a]	Oxidant	Catalyst loading[b] (mol%)	Oxidant/substrate molar ratio	Epoxide yield (%)[c]	TOF (h^{-1})
1	Catalyst-free	$C_2H_4Cl_2$	TBHP	–	2.24	–	–
2	$H_4SiW_{12}O_{40}$	$C_2H_4Cl_2$	TBHP	–	2.24	Trace	–
3	$H_3PW_{12}O_{40}$	$C_2H_4Cl_2$	TBHP	–	2.24	Trace	–
4	**1** (15)	CH_3OH	TBHP	0.90	1.24	17	3
5	**1** (15)	CH_3CN	TBHP	0.90	2.24	6	12.4
6	**1** (15)	CH_2Cl_2	TBHP	0.90	2.24	76	157
7	**1** (15)	$CHCl_3$	TBHP	0.90	2.24	79	163
8	**1** (15)	$C_2H_4Cl_2$	TBHP	0.90	2.24	99	206
9	**1** (15)	$C_2H_4Cl_2$	H_2O_2	0.90	2.24	52	107.4
10	**1** (15)	$C_2H_4Cl_2$	$H_2O_2{\cdot}CON_2H_4$	0.90	2.24	32	66
11	**1** (15)	$C_2H_4Cl_2$	$NaIO_4$[d]	0.90	2.24	Trace	–
12	**1** (15)	$C_2H_4Cl_2$	TBHP	0.90	2.24	99	206
13	**1** (10)	$C_2H_4Cl_2$	TBHP	0.60	2.24	99	309
14	**1** (7)	$C_2H_4Cl_2$	TBHP	0.42	2.24	72	318.6
15	**1** (5)	$C_2H_4Cl_2$	TBHP	0.30	2.24	39	242
16	**1** (10)	$C_2H_4Cl_2$	TBHP	0.60	2.24	99	309
17	**1** (10)	$C_2H_4Cl_2$	TBHP	0.60	1.68	70	216.7
18	**1** (10)	$C_2H_4Cl_2$	TBHP	0.60	1.12	31	96
19	**1** (10)	$C_2H_4Cl_2$	TBHP	0.60	0.56	28	86.7
20	**2** (20)	CH_3OH	TBHP	1.24	2.24	5	1.3
21	**2** (20)	CH_3CN	TBHP	1.24	2.24	4	1
22	**2** (20)	CH_2Cl_2	TBHP	1.24	2.24	32	8.3
23	**2** (20)	$CHCl_3$	TBHP	1.24	2.24	54	14
24	**2** (20)	$C_2H_4Cl_2$	TBHP	1.24	2.24	99	26
25	**2** (20)	$C_2H_4Cl_2$	H_2O_2	1.24	2.24	39	10
26	**2** (20)	$C_2H_4Cl_2$	$H_2O_2{\cdot}CON_2H_4$	1.24	2.24	18	4.7
27	**2** (20)	$C_2H_4Cl_2$	$NaIO_4$[d]	1.24	2.24	Trace	–
28	**2** (15)	$C_2H_4Cl_2$	TBHP	0.92	2.24	78	27
29	**2** (10)	$C_2H_4Cl_2$	TBHP	0.61	2.24	53	27.5
30	**2** (7)	$C_2H_4Cl_2$	TBHP	0.43	2.24	37	27.4
31	**2** (5)	$C_2H_4Cl_2$	TBHP	0.31	2.24	25	26
32	**2** (20)	$C_2H_4Cl_2$	TBHP	1.24	2.24	99	26
33	**2** (20)	$C_2H_4Cl_2$	TBHP	1.24	1.68	68	17.6
34	**2** (20)	$C_2H_4Cl_2$	TBHP	1.24	1.12	43	11.2
35	**2** (20)	$C_2H_4Cl_2$	TBHP	1.24	0.56	22	5.7

Reaction times are 30 min for catalyst **1**, and 180 min for catalyst **2**

[a] Amounts of solvent are 2 mL

[b] Calculated for 0.5 mmol cyclooctene

[c] GC yields are based on the starting cyclooctene

[d] Tetra-butyl phosphonium bromide was used as phase transfer reagent

was carried out using tert-Butyl hydroperoxide in different reaction media at refluxed conditions (Table 1). No product was obtained in the absence of any catalyst (Table 1, entry 1). The reaction was incomplete or exhibited extremely low catalytic activities in the presence of $H_4SiW_{12}O_{40}$ and $H_3PW_{12}O_{40}$ POMs homogeneous systems (Table 1, entry 2 and 3). The effects of different solvents (Table 1, entries 4–8), mg of catalyst (Table 1, entries 12–15), oxidant type (Table 1, entries 8–11), mol% for catalyst loading (0.3–0.9 mol%), and oxidant to substrate molar ratio (0.56–2.24 molar ratio) for **1** and **2** catalyst were investigated. The experiments show that with these catalysts, TBHP is the only oxidizing system, which can proceed the epoxidation of cyclooctene in $C_2H_4Cl_2$. Other oxygen sources such as hydrogen peroxide, sodium periodate (in the presence of 0.01 g tetra-butyl phosphonium bromide as phase transfer reagent) and urea-hydrogen peroxide in $C_2H_4Cl_2$ do not show any activity (Table 1, entries 8–11 and 23–26).

In order to study the effects of solvent, protic and aprotic solvents with different polarity and coordinating ability were used in epoxidation of cyclooctene with TBHP. The solvents of CH_3Cl, CH_2Cl_2, CH_3OH, CH_3CN and $C_2H_4Cl_2$ were used for oxidation of cyclooctene in the presence of tert-BuOOH (Table 1, entries 4–8 and 19–23). For EtOH and CH_3CN a detrimental effect on the reaction of cyclooctene was observed, giving less than 7% conversion at 30 min for catalyst **1** and 180 min for catalyst **2**. The observed catalytic activities do not correlate with the polar properties of the solvents. Instead, the coordinating ability of the solvent seems to have a major influence. Thus, the solvents EtOH and CH_3CN may compete with TBHP for connection to coordination sites on transition metal catalyst. According to the results 1,2-dichloroethane showed the highest conversion rates as the solvent.

In the next step, to optimize the reaction time the reflux was performed at different times 10, 20, 30, 60, 90, 120,150,180 min. Figure 10 shows the effect of reaction time on epoxidation of cyclooctene with TBHP. A comparison reactivity of catalyst **1** and catalyst **2** reveals that **1** is more reactive and after 30 min its conversion reaches to maximum and becomes constant. However, catalyst **2** needs 3 h to reach this point.

The ratio of oxidant to substrate is one of the most crucial parameters in catalytic epoxidation processes. Different values of 0.1, 0.2, 0.3 and 0.4 mmol were selected for the oxidant. The results in (Table 1, entries 16–19 and 32–35) for **1** and **2** respectively, show that the optimum ratio of oxidant to substrate for catalyst **1** and catalyst **2** is 2.24. In order to select a right value of catalyst, we checked out values of 20, 15, 10 and 7 mg (Table 1, entries 12–15 and 28–31). The highest conversion rate for **1** and **2** were 10 and 20 mg respectively. The reaction temperature was also optimized by carrying out the reaction in 90 °C and room temperature. At room temperature (25 °C), the product yields were low for compound **2** but the catalyst **1** showed 15% conversion. By increasing the reaction temperature to 90 °C the conversion was improved for both samples. Generally, catalytic reactions are considered to take place at the surface of catalysts. In the low temperature section, the reactants are not easy to reach the catalyst surface, so an increase in conversion is observed as the temperature goes up until the chemical turnover at the surfaces is equal to the chemical reaction rate on their surfaces. After that, the conversion does not alter with temperature due to the fact that catalysts do not have sufficient exposed surface area for the reactants to carry out high rates of catalytic reactions. With the viewpoint of practical production, the optimum reaction temperature was fixed at 90 °C for further studies.

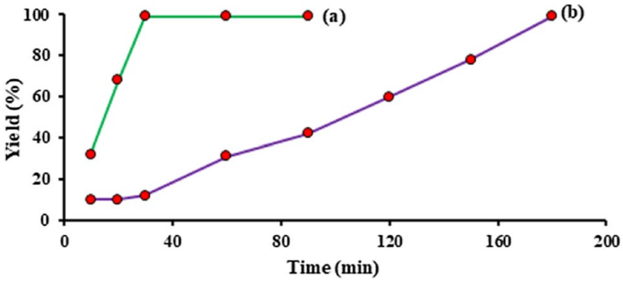

Fig. 10 Epoxidation of 0.5 mmol cis-cyclooctene with 1.12 mmol TBHP catalyzed by *a* 10 mg of **1** or *b* 20 mg of **2** in 2 mL $C_2H_4Cl_2$ under refluxed conditions

According to these data catalyst **1** as nanocatalyst gave the highest yield in 10 mg of catalyst, $C_2H_4Cl_2$ as solvent, 0.6 mol% for catalyst loading, and 2.24 molar ratios for oxidant to substrate (Table 1, entry 13). In the case of catalyst **2**, these values in $C_2H_4Cl_2$ are 20 mg of catalyst, 1.24 mol% for catalyst loading, and 2.24 molar ratios for oxidant to substrate (Table 1, entry 24). Therefore, catalyst **1** exhibits a more efficient activity in the epoxidation process. The high catalytic activity of **1** in epoxidation reaction of olefins is probably due to the less reduction potential of this compound [50].

Finally epoxidation of several olefins including linear, cyclic and phenyl-substituted olefins with tert-Butyl hydroperoxide as oxidant were carried out in the presence of **1** and **2** as nanocatalyst in refluxed conditions. The expected products were obtained with various yields (Table 2). For all substrates, catalyst **1** behaves as a better catalyst than catalyst **2**. For epoxidation of styrene, the conversions are found to be 87.0 and 85.0% with excellent selectivity for epoxide formation in the presence of both catalyst **1** and **2**, respectively. Aside from epoxide, benzaldehyde has been detected as the minor product for these reactions. For the epoxidation of cyclohexene, the conversions are approximately 99.0 and 98.0% with high selectivity for epoxide formation in the presence of catalyst **1** and **2**, respectively. Apart from epoxide, 2-cyclohexen-1-ol and 2-cyclohexen-1-one are the other by-products formed during the reaction. 1-Octene and 1-Hexen shows low yield in the epoxidation reaction (Table 2, entry 3 and 4). The results show that electron-rich alkenes are more reactive than other alkenes. According to the epoxidation mechanism suggested earlier, we can also see that electron-rich alkenes are more reactive than other alkenes [51]. Consequently, cyclooctene and cyclohexene with cyclic structure

Table 2 Epoxidation of some olefins with TBHP catalyzed by **1** and **2** in refluxed conditions

Entry	Alkene	Catalyst **1**[a]				Catalyst **2**[a]			
		Conversion (epoxide)[a] (%)	Selectivity (%)	Time (min)	TOF (h^{-1})	Conversion (epoxide)[a] (%)	Selectivity (%)	Time (h)	TOF (h^{-1})
1	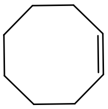	99 (99)	100	30	309	98 (98)	100	3	26
2	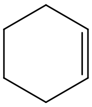	99 (91)[b]	92	30	309	98 (87)	88.77	3	26
3	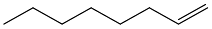	54 (54)	100	90	55.7	48 (48)	100	5	7.5
4		61 (61)	100	90	63	56 (56)	100	5	8.7
5	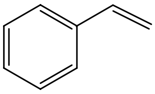	87 (82)[c]	94.25	90	89.8	85 (75)	88.37	4	16.5
6	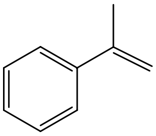	92 (85)[d]	92.39	60	142.4	90 (81)	90	3.5	20
7	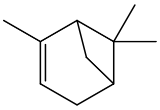	87 (80)	92	60	134.7	82 (75)	91.46	3.5	18.2
8	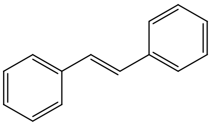	95 (95)[e]	100 (trans)[f]	60	147	95 (95)[e]	100 (trans)[f]	6	12.3
9	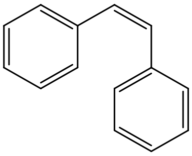	(90)[e]	80 (cis), 10 (trans)[g]	60	139.3	(86)[e]	75 (cis), 11 (trans)[g]	6	11.2

Reaction conditions: alkene (0.5 mmol), TBHP (1.12 mmol), catalyst **1** (10 mg), catalyst **2** (20 mg), $C_2H_4Cl_2$, (2 mL)

[a] GC yield based on the starting alkenes

[b] The by-products are 8% for catalyst **1** and 11% for catalyst, **2**

[c] The by-product are 5% for catalyst **1** and 10% for catalyst, **2**

[d] The by-product are 7% for catalyst **1** and 9% for catalyst, **2**

[e] Both ^{1}H NMR and GC data approved the reported yields

[f] Trans isomer is only product according to ^{1}H NMR data

[g] Cis and trans isomers are produced according to ^{1}H NMR data

Table 3 Catalytic activity of various catalysts for the epoxidation of cyclooctene

Entry	Catalyst	Substrate	Solvent	Time (h)	TOF (h^{-1})	Conv. (%)	Sel. (%)	References
1	**1**	Cyclooctene	$C_2H_4Cl_2$	0.5	309	99	100	This work
2	**2**	Cyclooctene	$C_2H_4Cl_2$	3	26	98	100	This work
3	[Ni(salen)-POM]	Cyclooctene	CH_3CN	6	6.4	77	28	[52]
4	PVMo-MCM/IBA/O_2	Cyclooctene	$C_2H_4Cl_2$	24	–	63	100	[53]
5	$[As_8V_{14}O_{42}(H_2O)][Cu(2,2'\text{-bpy})_2]_4$	Cyclooctene	CH_3CN	9	–	65.4	100	[54]
6	$[As_8V_{14}O_{42}(H_2O)][Cu(1,10\text{-phen})_2]_4$	Cyclooctene	CH_3CN	9	–	33	100	[54]
7	Au/BW11/Al_2O_3	Cyclooctene	$C_2H_4Cl_2$:CH_3CN	24	–	53	97.0	[55]

display more activities than 1-hexene and 1-octene, which contain terminal double bonds. The epoxidation reaction of trans-stilbene has remarkable selectivity with excellent conversion efficiency whereas, the epoxidation of cis-stilbene give a mixture of cis- and trans-stilbene oxide with high cis/trans epoxide ratio (Table 2 entry 8 and 9). It is obvious that electron rich olefins are more reactive than electron poor ones.

3.3.1 Comparison with Other Catalysts

The comparison of catalysts **1** and **2** with previously offered catalysts in the epoxidation of cyclooctene are given in Table 3. Mirkhani et al. have demonstrated that the epoxidation of cyclooctene could be done with Ni(salen)–POM complex [52]. They performed the epoxidation reaction in acetonitrile as a solvent and reported 77% conversion and 28% selectivity in epoxidation of cyclooctene (Table 3, entry 3). In addition, Khenkin et al. carried out the epoxidation of alkenes by PVMo-MCM/IBA/O_2 in 1,2-dichloroethane (Table 3, entry 4) [53]. Moreover, Guo et al. found out that two complexes $[As_8V_{14}O_{42}(H_2O)][Cu(2,2'\text{-bpy})_2]_4$ and $[As_8V_{14}O_{42}(H_2O)][Cu(1,10\text{-Phen})_2]_4$ could be applied to the selective epoxidation of olefins (Table 3, entries 5 and 6) [54]. Furthermore, Jameel et al. have reported that Au/BW_{11}/Al_2O_3 used as true heterogeneous catalyst, could be recycled three times without loss of activity (Table 3, entry 7) [55]. In the present work, the **1** gives 99% conversion and 100% selectivity and **2** shows 98% conversion and 100% selectivity for epoxidation cyclooctene (Table 3, entries 1 and 2). Therefore, the present catalysts display the desirable catalytic activity for the epoxidation of alkenes compared to other catalysts listed in Table 3.

3.3.2 Catalysts Recycling

The catalyst recovery and reusability are the two most important features for many catalytic processes. The reusability of catalyst **1** and **2** were investigated for oxidation of cis-cyclooctene as a model reaction using tert-Butyl hydroperoxide at optimum conditions. In each experiment, after completion the reaction, the catalysts were easily separated by centrifugation, washed several times with 1,2-dichloroethane, dried, and then reused in the subsequent experiments under the same conditions. The recovered catalyst showed an efficient recycling ability without giving any change in the reaction time and the yield of the product. The heterogenic character of these catalysts was checked by the hot filtration test. Because of this reason, each catalyst was removed by centrifuging the catalytic mixture in the middle of the optimization process, and the manner was continued to reach an optimum time of reaction completion. The obtained results showed that when the catalyst was removed from the reaction medium, the catalytic procedure stopped and did not continue anymore. This test proves that the catalytic reactions are retained in heterogeneous conditions, and the catalysts are not leached to the reaction medium. Furthermore, ICP has been employed to detect/determine the amount of metal that leached out into the reaction mixture. No detectable molybdenum was found in the reaction mixtures. The obtained results revealed that the amount of Mo in catalyst **1** after six runs decreased to 3.06% and in catalyst **2** decrease to 3.05%. Moreover, the IR spectra of recovered catalysts did not show any obvious differences with fresh catalysts (Fig. 11). The structural integrity of the recovered catalyst was confirmed by XRD analysis. As shown in Fig. 12, the basic lattice structure of **1** and **2** nanocatalysts were not altered after six cycles. The results are given in Table 4. As shown in Fig. 13 the recovered catalysts were reused at least six times without losing of activity.

4 Conclusions

In this study, we have successfully prepared two nanohybrid heterogeneous catalysts by anchoring molybdenylacetylacetonate complex and Schiff base with polyoxometalates. These catalysts characterized with routine

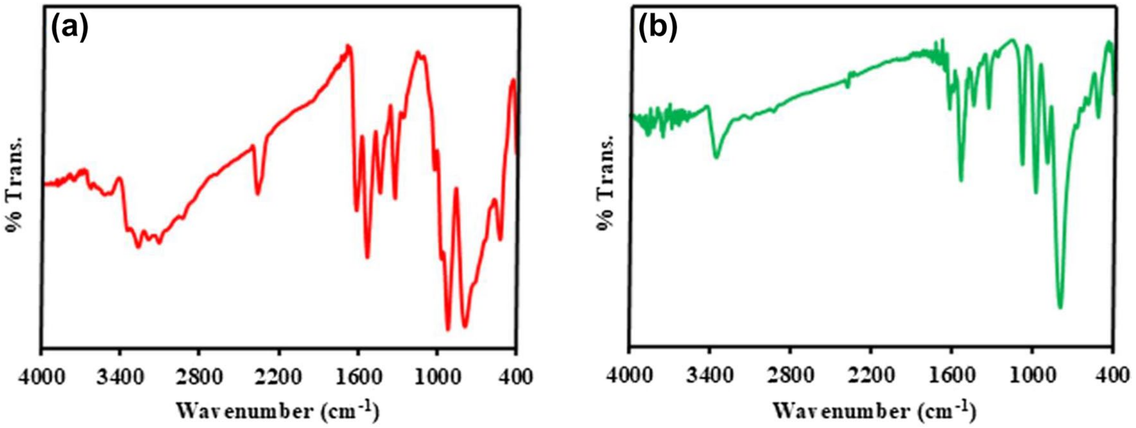

Fig. 11 The FT-IR spectra of recovered **a** **1** and **b** **2** nanocatalysts

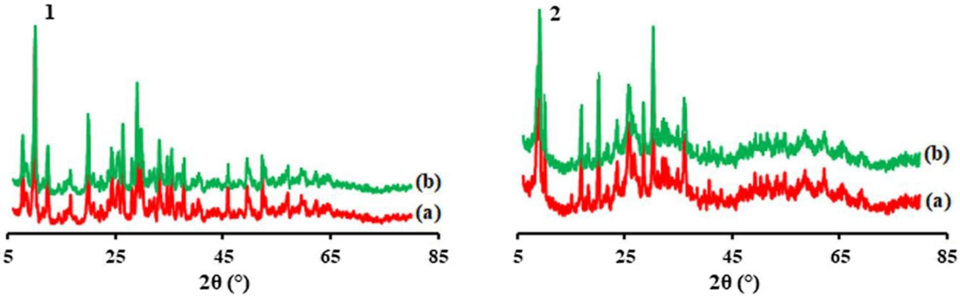

Fig. 12 The XRD pattern of **1** and **2** nanocatalysts: *a* basic XRD pattern and *b* after six cycles

Table 4 Epoxidation of cis-cylooctene with TBHP in refluxed conditions using recycled catalysts

Number of cycle	Catalyst **1**[a]		Catalyst **2**[a]	
	Epoxide yield[b] (%)	TOF (h^{-1})	Epoxide yield[b] (%)	TOF (h^{-1})
1	98	306.25	97	25.26
2	96	300	95	24.73
3	95	296.88	94	24.48
4	93	290.62	94	24.48
5	93	290.62	93	24.22
6	91	284.38	90	23.44

[a] Reaction condition: 0.5 mmol cyclooctene, 1.12 mmol TBHP, 10 mg catalyst **1** and 20 mg catalyst **2**, 2 mL $C_2H_4Cl_2$, 30 min for catalyst **1** and 180 min for catalyst **2**

[b] GC yields are based on the starting cyclooctene

techniques. We have found that the catalytic activity of a [MoO_2(acac)$_2$] complex can be improved by creation of hybrid combinations with lacunary Keggin-type polyoxometalates. Such catalytic systems combine the advantages of biphasic and heterogeneous catalysis as they allow an easy separation of products and catalysts, without their drawbacks (e.g. high reaction time and catalyst leaching). The catalyst **1** shows a better catalytic activity than **2**. The new heterogeneous nanocatalysts could be easily recovered by centrifuge and reused at least six times without significant loss of activity. These nanocatalysts display good and desirable catalytic activity in the epoxidation of various olefins under quite heterogeneous conditions compared to other reported catalysts.

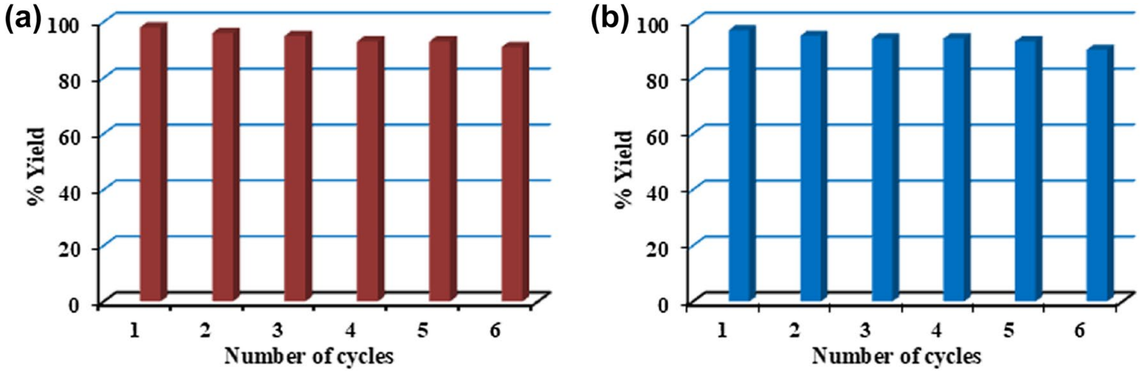

Fig. 13 The recycling experiment of **a** catalyst **1** and **b** catalyst **2** for oxidation of cis-cyclooctene at optimum conditions

References

1. Mizuno N, Kamata K (2011) Coord Chem Rev 255:2358
2. Pathare SP, Akamanchi KG (2013) Tetrahedron Lett 54:6455
3. Maksimchuk NV, Timofeeva MN, Melgunov MS, Shmakov AN, Chesalov YA. Dybtsev DN, Fedin VP, Kholdeeva OA (2008) J Catal 257:315
4. Conte V, Floris B (2010) Inorg Chim Acta 363:1935
5. Brocas AL, Mantzaridis CH, Tunc D, Carlotti S (2013) Prog Polym Sci 38:845
6. Simonneaux G, Le Maux P, Ferrand Y, Rault-Berthelot J (2006) Coord Chem Rev 250:2212
7. Cancino P, Paredes-García V, Aguirre P, Spodine E (2014) Catal Sci Technol 4:2599
8. Luts T, Frank R, Suprun W, Fritzsche S, Hey-Hawkins E, Papp H (2007) J Mol Catal A 273:250
9. Xia QH, Ge HQ, Ye CP, Liu ZM, Su KX (2005) Chem Rev 105:1603
10. Long DL, Burkholder E, Cronin L (2007) Chem Soc Rev 36:105
11. Nyman M (2011) Dalton Trans 40:8049
12. Compain JD, Mialane P, Dolbecq A, Mbomekallé IM, Marrot J, Sécheresse F, Rivière E, Rogez G, Wernsdorfer W (2009) Angew Chem Int Ed 48:3077
13. Duan CY, Wei ML, Guo D, He C, Meng QJ (2010) J Am Chem Soc 132:3321
14. Coronado E, Giménez-Saiz C, Gómez-García CJ (2005) Coord Chem Rev 249:1776
15. Zhao JW, Shi DY, Chen LJ, Li YZ, Ma PT, Wang JP, Niu JY (2012) Dalton Trans 41:10740
16. Fukaya K, Yamase T (2003) Angew Chem Int Ed 42:654
17. Chen LJ, Shi DY, Zhao JW, Wang YL, Ma PT, Wang JP, Niu JY (2011) Cryst Growth Des 11:1913
18. Mitchell SG, Streb C, Miras HN, Boyd T, Long DL, Cronin L (2010) Nat Chem 2:308
19. Yin P, Wu P, Xiao Z, Li D, Bitterlich E, Zhang J, Cheng P, Vezenov DV, Liu T, Wei Y (2011) Angew Chem Int Ed 50:2521
20. Fang XK, Anderson TM, Hill CL (2005) Angew Chem Int Ed 44:3540
21. Mizuno N, Misono M (1998) Chem Rev 98:199
22. Pope MT, Muller A (1991) Angew Chem Int Ed 30:34
23. Wang L, Feng Z, Cai H (2009) J Electroanal Chem 636:36
24. Keggin JF (1933) Nature 131:908
25. Zhao S, Jia Y, Song YF (2013) Appl Catal A 453:188
26. Jahier C, Mal SS, Al-Oweini R, Kortz U, Nlate S (2013) Polyhedron 57:57
27. Zhang Z, Zhang F, Zhu Q, Zhao W, Ma B, Ding Y (2011) J Colloid Interface Sci 360:189
28. Sousa JLC, Santos ICMS., Simões MMQ, Cavaleiro JAS, Nogueira HIS, Cavaleiro AMV (2011) Catal Commun 12:459
29. Balula SS, Santos ICMS., Cunha-Silva L, Carvalho AP, Pires J, Freire C, Cavaleiro JAS, de Castro B, Cavaleiro AMV (2013) Catal Today 203:95
30. Hill CL, Prosser-McCartha CM (1995) Coor Chem Rev 143:407
31. Kozhevnikov IV (1995) Catal Rev Sci Eng 37:311
32. Proust A, Matt B, Villanneau R, Guillemot G, Gouzerh P, Izzet G (2012) Chem Soc Rev 41:7605
33. Izzet G, Ishow E, Delaire J, Afonso C, Tabet JC, Proust A (2009) Inorg Chem 48:11865
34. Izarova NV, Vankova N, Heine T, Biboum RN, Keita B, Nadjo L, Kortz U (2010) Angew Chem Int Ed 49:1886
35. Cao GJ, Liu JD, Zhuang TT, Cai XH, Zheng ST (2015) Chem Commun 51:2048
36. Gouzerh P, Proust A (1998) Chem Rev 98:77
37. Uchida S, Mizuno N (2007) Coord Chem Rev 251:2537
38. Ren Y, Wang M, Chen X, Yue B, He H (2015) Materials 8:1545
39. Aany Sofia LT, Krishnan A, Sankar M, Kala Raj NK, Manikandan P, Rajamohanan PR, Ajithkumar TG (2009) J Phys Chem C 113:21114
40. Yamaguchi K, Yoshida C, Uchida S, Mizuno N (2005) J Am Chem Soc 127:530
41. Kovalchuk T, Sfihi H, Zaitsev V, Fraissard J (2007) J Catal 249:1
42. Chen GJJ, Mcdonald JW, Newton WE (1976) Inorg Chem 15:2612
43. Channa AM, Siyal AlN, Memon SQ, Parveen S (2014) Desalin Water Treat 52:3664
44. Tayyari SF, Milani nejad (2000) Spectrochim Acta A 56:2679
45. Rocchiccioli-Deltcheff C, Thouvenot R, Franck R (1976) Spectrochim Acta A 32:587
46. Anbarasu G, Malathy M, Karthikeyan P, Rajavel R (2017) J Solid State Chem 253:305
47. Williamson GK, Hall WH (1953) Acta Metall 1:22
48. Grama L, Boda F, Gaz Florea AS, Curticăpean A, Muntean DL (2014) Acta Medica Marisiensis 60:84
49. Farias M, Martinelli M, Rolim GK (2011) Appl Catal A 403:119
50. Zonoz FM (2016) Electrocatalysis 7:215
51. Cornils B, Hermann WA (1996) Applied homogeneous catalysis with organometallic compounds, vol 2.Wiley, Weinheim, p 636
52. Mirkhani V, Moghadam M, Tangestaninejad S, Bahramian B (2008) Catal Commun 9:2171
53. Khenkin AM, Neumann R, Sorokin AB (1999) Catal Lett 63:189
54. Guo HY, Li ZF, Zhao DC, Hu YY, Xiao LN, Cui XB, Guan JQ, Xu JQ (2014) Cryst Eng Comm 16:2251
55. Jameel U, Zhu M, Chen X (2016) J Zhejiang Univ Sci A 17:1000